Two-soliton precession state in a parametrically driven magnetic wire

D. Urzagasti,[1] D. Laroze,[1,2] M. G. Clerc,[3] S. Coulibaly,[4] and H. Pleiner[2,a)]
[1]*Instituto de Alta Investigación, Universidad de Tarapacá, Arica, Chile*
[2]*Max Planck Institute for Polymer Research, Mainz, Germany*
[3]*Departamento de Física, FCFM, Universidad de Chile, Santiago, Chile*
[4]*Laboratoire de Physique des Lasers, Atomes et Molécules, Université des Sciences et Technologies de Lille, Villeneuve d'Ascq Cedex, France*

The pattern formation in a magnetic wire forced by a time dependent magnetic field is studied. This system is described in the continuum limit by the Landau-Lifshitz-Gilbert equation. The spatio-temporal magnetization field exhibits two-soliton bound state solutions. Close to the parametric resonance instability, an amplitude equation allows us to understand and characterize these localized states. © *2012 American Institute of Physics*. [doi:10.1063/1.3672872]

Solitons in magnetism have been intensely studied in the past decades due to trheir potential technological applications. The state of the art for conservative and for dissipative systems can be found in Refs. 1 and 2. Here, we deal with a dissipative system. Such systems can have spatially localized, stable, and dynamic excitations. Such a dynamic structure, appearing in a restricted spatial region and asymptotically connecting time-independent states in the rest of the space, are called solitons.[3] Recently, experimental results of dissipative solitons in magnetic systems have been obtained.[4,5] In addition to ordinary single soliton solutions, we find other localized states in the form of bound solitons, called two-soliton solutions. Such dissipative states have been theoretically obtained in generic parametrically driven systems[6] and experimentally observed in hydrodynamic[7] or electro-mechanical systems,[8] just to mention a few.

First, we report upon the numerical observation of parametrically excited two-soliton states in an easy-plane ferromagnetic wire subject to a combined, constant, and oscillatory applied magnetic field. It is well-known that, close to the parametric resonance, the dynamics of this system can be qualitatively described by a (parametrically driven, damped) nonlinear Schrödinger equation.[2] This equation allows us, in a second step, to understand and further characterize these two-soliton states. In particular, we show numerically that this equation indeed has two-soliton solutions in a phase space region similar to what we have found by the direct numerical procedure in the first part. In addition, we derive, from the nonlinear Schrödinger equation, approximate analytical expressions for the bound two-soliton states and provide the range of parameters where these localized structures exist.

We consider the continuum dynamics of the magnetization, $\mathbf{m} = \mathbf{m}(z, t)$, of an anisotropic wire. Throughout this manuscript we use dimensionless quantities having scaled the magnetization (and magnetic fields) by the saturation magnetization, M_s, the time, t, by $1/|\gamma|M_s$, where γ is the gyromagnetic factor associated with the electron spin, $|\gamma_e|\mu_0$, and the space coordinate, z, by the exchange length, $l_{ex} = \sqrt{2J/\mu_0 M_s^2}$, where J is the effective exchange coupling constant. Taking, e.g., material values,[9] $M_s \sim 800$ kA/m or $\mu_0 M_s \sim 1$T, and $|\gamma| \approx 2.21 \times 10^5$ m A^{-1} s^{-1}, the dimensionless time scale corresponds to $\approx$6 ps as a physical scale. The present technology is able to follow experiments at the femtosecond scale. Indeed, Beaurepaire *et al.*[10] were the first to observe the spin dynamics at a time-scale below the picosecond scale in nickel particles.

The dynamical evolution of the magnetization can be modeled by the Landau-Lifshitz-Gilbert equation,[3]

$$\partial_t \mathbf{m} - \lambda \mathbf{m} \times \partial_t \mathbf{m} = -\mathbf{m} \times \Gamma. \tag{1}$$

The effective torque field, $\Gamma = \partial_z^2 \mathbf{m} - \beta(\mathbf{m} \cdot \hat{\mathbf{z}})\hat{\mathbf{z}} + \mathbf{H}$, contains the Laplacian term that accounts for the coupling of the magnetization with the first neighbors; $\beta(>0)$ is the easy-plane anisotropy constant, λ stands for the Gilbert damping constant, and $\mathbf{H}$ is the external magnetic field. We consider an external magnetic field that comprises a constant and an oscillatory part, which are both perpendicular to the wire axis, $\mathbf{H} = (H_0 + h_0 \cos \Omega t)\hat{\mathbf{x}}$.

Let us briefly review some previous results. A simple homogeneous solution of model (1) is $\mathbf{m} = \hat{\mathbf{x}}$, which becomes unstable against homogeneous oscillations at $h_{0c}^2 = (4\Omega_0)^2[\nu^2 + (\lambda q/2)^2]/\beta^2$, if the system is forced at the frequency, $\Omega_c = 2(\Omega_0 + \nu)$, with $\Omega_0 = \sqrt{H_0(H_0 + \beta)}$, $q = 2H_0 + \beta$, and ν being the detuning parameter.[3] This instability is a parametric resonance and the relationship for h_{0c} defines the first Arnold tongue. In addition, the system admits single soliton solutions,[2] with the localized structures exhibiting a single bump. These solitons appear below the Arnold tongue and for the negative detuning values.

Apart from the standard soliton solution, numerically we found other types of localized structures by directly solving Eq. (1). In particular, the system exhibits a stable two-soliton solution, where the localized dynamic structure exhibits two bumps. Figure 1 shows the y component of the magnetization field as a function of space and time in the

a)Electronic mail: pleiner@mpip-mainz.mpg.de.
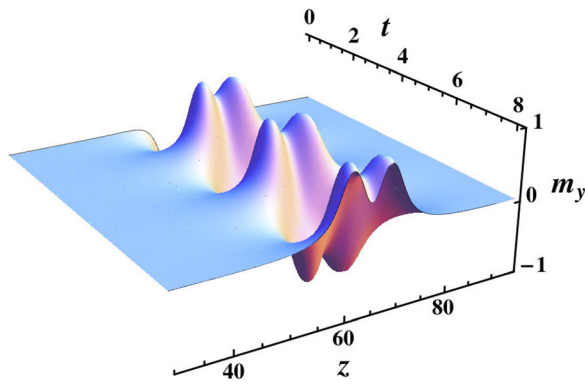
FIG. 1. (Color online) The m_y as a function of the space and time in a two-soliton solution for $\lambda = 0.015$, $H_0 = 3$, $\beta = 20$, $\nu = -0.398$, and $h_0 = 0.6$.

stable two-soliton region. The latter is shown in red (filled squares) in Fig. 2, which is the soliton phase diagram in the ν and h_0 space. The existence range of single solitons (blue, open circles) is larger and expands into more negative detuning values. In order to build this phase diagram, we start, as an initial condition, with two separate single solitons and determine their final stationary state. They either decay (no soliton), merge completely into one single soliton, or form a bound pair of solitons with a fixed distance between them (the two-soliton state). The existence range of these solutions is robust against starting with different finite amplitude initial conditions. This is shown in Fig. 3, where more general dynamic perturbations are chosen as initial conditions and the same final states are obtained.

Due to the complexity of model (1) only fully numerical solutions are possible. To gain more insight, in a second step we study these localized states by an amplitude equation, which is, mathematically, quite simpler. Close to the parametric instability, it can systematically be derived from the full dynamic equations[3] and generally gives a qualitatively correct description, although often a quantitative agreement is not obtained.[11] Indeed, we show in the following text that two-soliton solutions are also found from the amplitude equation and we give an approximate analytical expression for them. The amplitude equation that describes our magnetic system close to the parametric resonance is the para-
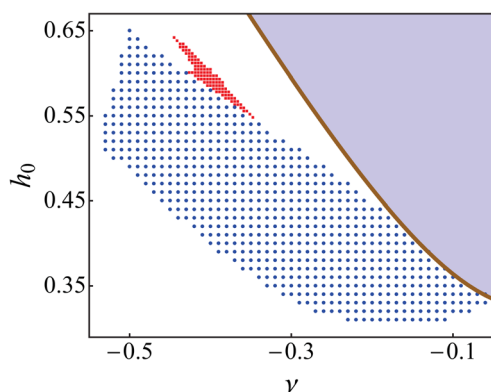
FIG. 2. (Color online) The existence region of solitons in the h_0 (field amplitude), and ν (detuning parameter) phase diagram of Eq. (1) for $\lambda = 0.015$, $H_0 = 3$, and $\beta = 20$. Open (blue) circles denote single soliton solutions, while filled (red) squares represent the bound two-soliton states.
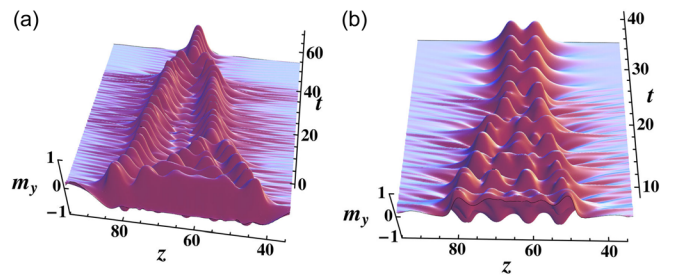
FIG. 3. (Color online) Space-time plot of m_y with (a) a single soliton, and (b) a two-soliton as the final state for $h_0 = 0.5$ and $h_0 = 0.6$, respectively. The fixed parameters are as in Fig. 2.

metrically driven and damped nonlinear Schrödinger equation (PDDNLS).[2] It is a partial differential equation for the complex amplitude, A, for the envelope of the oscillations, $m_z(t,z) = A(T,Z)\exp(i(\Omega_0 + \nu)t) + c.c. + \Sigma(A,t)$, where $c.c.$ signifies the complex conjugate and $\Sigma(A,t)$ is a small correction function in the form of a polynomial series in A. One finds, after some lengthy calculations, the following solvability condition:[2]

$$\partial_T A = -i\nu A - i|A|^2 A - i\partial_Z^2 A - \mu A + \alpha A^*, \qquad (2)$$

where A^* is the complex conjugate of A. It describes the dynamics of the envelope amplitudes in the long time and large space scale through $T \equiv \alpha t$ and $Z \equiv \sqrt{2\Omega_0/q}\, z$, respectively. Equation (2) is the PDDNLS equation with an effective damping, $\mu = \lambda q/2$, and driving parameter, $\alpha = h_0 q/(4\Omega_0)$. This equation has different homogeneous states, of which the simplest one is $A = 0$, representing a constant magnetization along the external field direction ($\mathbf{m} = \hat{\mathbf{x}}$). Single solitons are among the non-trivial steady states of Eq. (2).[2] Other solutions of the PDDNLS equation and their properties can be found in Refs. 3 and 6. In Fig. 4(a) we show the phase diagram containing not only single solitons, but also bound two-soliton states, which we obtained b numerically by solving Eq. (2) when the initial conditions are two separated single soliton solutions. The topology of this phase diagram is similar to that obtained in Fig. 1 by using Eq. (1). As expected, there are differences on the quantitative level.

One advantage of using the amplitude equation instead of the full dynamic one is the possibility to derive (approximate) analytical solutions from the former. Separating the real and the imaginary part of the amplitude, $A = u + iv$, we obtain,

$$\begin{aligned}\partial_T u &= (\alpha - \mu)u + \nu v + \partial_Z^2 v + \mathcal{N}v, \\ \partial_T v &= -\nu u - (\alpha + \mu)v - \partial_Z^2 u - \mathcal{N}u,\end{aligned} \qquad (3)$$

where $\mathcal{N} = u^2 + v^2$. The non-trivial steady single soliton solutions are $u_S = \eta_{++}\,\mathrm{sech}\,\xi$ and $v_S = \eta_{--}\,\mathrm{sech}\,\xi$, where $\eta_{\pm\pm} = \pm k\sqrt{1 \pm \mu/\alpha}$ and $\xi = kZ$ with $k^2 = \sqrt{\alpha^2 - \mu^2} - \nu$. Note that k^{-1} accounts for the soliton width; the stability conditions of these solitons can be found in Refs. 2 and 12.

Due to the nonlinear nature of the underlying equations, two single soliton solutions, some distance apart, generally feel an effective interaction.[6,7] This makes it possible that bound soliton states exist. In order to derive an approximate
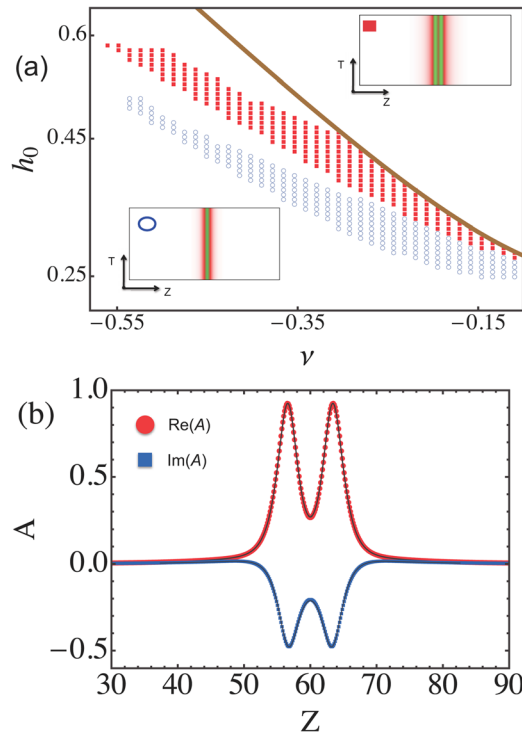
FIG. 4. (Color online) (a) The $\nu - h_0$ phase diagram of the existence of different soliton states of Eq. (2). The open (blue) circles represent single solitons, while the filled (red) squares denote two-soliton bound states, respectively. The solid line is $\alpha^2 = \mu^2 + \nu^2$, where the spatial extensions of the solitons shrinks to zero. The insets show the spatio-temporal behavior of the real part of A for both types of solitons. (b) Spatial distribution of the amplitude of a two-soliton solution; the lines are approximate analytical results from Eq. (5), while the dots represent the numerical solution of Eq. (2) at $h_0 = 0.5$, $\nu = -0.4$, and $\Delta = 6.8$. The fixed parameters are as in Fig. 2. The connection of α and μ of Eq. (2) with the magnetic parameters is given in the text.

solution of these bound states we consider two, initially well separated, single solitons, whose distance (between the respective maxima) is larger than the typical soliton width. Hence, we can write $u = u_S(\zeta_+) + u_S(\zeta_-) + \delta u$ and $v = v_S(\zeta_+) + v_S(\zeta_-) + \delta v$ for the two fields, with $\mathcal{O}(\delta u^2) \sim \mathcal{O}(\delta v^2) \ll 1$, meaning the effective interaction is small. Here, $\zeta_\pm = \xi \pm \Delta/2$, where Δ is the distance between the two maxima. Inserting this ansatz into the equations for (u, v) and linearizing the equations for $(\delta u, \delta v)$ in the stationary case we obtain,

$$
\begin{aligned}
d^2\delta u/d\xi^2 + (b_{++} - 1)\delta u + \eta b_{-+}\,\delta v &= c_+, \\
d^2\delta v/d\xi^2 + (b_{+-} - 1)\delta v + \eta^{-1}b_{--}\,\delta u &= c_-,
\end{aligned}
\tag{4}
$$

using the abbreviations $c_\pm = -6S\eta_{\pm\pm}\,\mathrm{sech}\,\zeta_-\,\mathrm{sech}\,\zeta_+$ and $b_{\pm\pm} = 3S^2 \pm ([1\pm 2\mu/\xi]S^2 + 1 + \nu/k^2)$ with $S \equiv \mathrm{sech}\,\zeta_- + \mathrm{sech}\,\zeta_+$ and $\eta \equiv \eta_{++}/\eta_{--}$. Approximate solutions of this

non-autonomous system of equations can be found by choosing a particular set of trial functions and optimizing the parameters with the result,

$$
\begin{aligned}
\delta w(\xi) \approx{}& a_0^w \Phi(\xi) + a_1^w \Phi(\xi)^2 + a_2^w \Phi(\xi)^4 \\
&+ a_3^w [1 - \Phi(\xi)]^2 \mathrm{sech}(a_4^w \xi),
\end{aligned}
\tag{5}
$$

where $w \in \{u, v\}$ and $\Phi(\xi) = (1/2)(\tanh \zeta_+ - \tanh \zeta_-)$. Thus, δu and δv have the same functional form, but different coefficients, $\{a_n^u\}$ and $\{a_n^v\}$, which are complicated functions of the parameters μ, ν, α, and Δ. In Fig. 4(b), the two-soliton state is shown by dots, based on a numerical solution of Eq. (2), and by lines, obtained from the approximate analytical solution (5). The comparison shows good agreement, with a difference of less than 5%.

In summary, we have determined the parameter region where two-soliton precession states occur in an anisotropic magnetic wire simultaneously exposed to a constant and a time dependent magnetic field. We have derived an approximate analytical solution for the stationary bound state, which is in good agreement with the numerical simulations. In closing, we mention that there exist even more complicated bound soliton states in this system such as, e.g., oscillating breather-like two-solitons and anti-symmetric stationary two-solitons. Work on these structures is in progress.

[1]A. M. Kosevich, W. A. Ivanov, and A. S. Kovalev, Phys. Rep. **194**, 117 (1990).

[2]I. V. Barashenkov, M. M. Bogdan, and V. I. Korobov, Europhys. Lett. **15**, 113 (1991).

[3]M. G. Clerc, S. Coulibaly, and D. Laroze, Europhys. Lett. **90**, 38005 (2010); Phys. Rev. E **77**, 056209 (2008); Int. J. Bifurcation Chaos Appl. Sci. Eng. **19**, 2717 (2009); Int. J. Bifurcation Chaos Appl. Sci. Eng. **19**, 3525 (2009); Physica D **239**, 72 (2010), and references therein.

[4]A. B. Ustinov et al., Phys. Rev. Lett. **106**, 017201 (2011); A. B. Ustinov et al., Phys. Rev. B **81**, 180406 (2010); A. B. Ustinov et al., Phys. Rev. B **80**, 052405 (2009).

[5]D. Koumoulis et al., Phys. Rev. Lett. **104**, 077204 (2010).

[6]I. V. Barashenkov and E. V. Zemlyanaya, Phys. Rev. E **83**, 056610 (2011); I. V. Barashenkov, E. V. Zemlyanaya, and T. C. van Heerden, Phys. Rev. E **83**, 056609 (2011), and references therein.

[7]W. Wang, X. Wang, J. Wang, and R. Wei, Phys. Lett. A **219**, 74 (1996).

[8]E. Kenig, B. A. Malomed, M. C. Cross, and R. Lifshitz, Phys. Rev. E **80**, 046202 (2009).

[9]I. D. Mayergoyz, G. Bertotti, and C. Serpico, *Nonlinear Magnetization Dynamics in Nanosystems* (Elsevier, Dordrecht, 2009).

[10]E. Beaurepaire, J. C. Merle, A. Daunois, and J. Y. Bigot, Phys. Rev. Lett. **76**, 4250 (1996).

[11]M. C. Cross and P. C. Hohenberg, Rev. Mod. Phys. **65**, 851 (1993).

[12]M. G. Clerc, S. Coulibaly, N. Mujica, R. Navarro, and T. Sauma, Philos. Trans. R. Soc. London, Ser. A **367**, 3213 (2009).